Pramana – J. Phys. (2020) 94:10
https://doi.org/10.1007/s12043-019-1896-y
© Indian Academy of Sciences

Rogue wave solutions of the chiral nonlinear Schrödinger equation with modulated coefficients

L FERNAND MOUASSOM*, ALAIN MVOGO and C BIOUELE MBANE

Department of Physics, Faculty of Science, University of Yaounde I, P.O. Box 812, Yaoundé, Cameroon
*Corresponding author. E-mail: layon32@yahoo.com

MS received 14 May 2019; revised 9 October 2019; accepted 4 November 2019

Abstract. The research of rogue wave solutions of the nonlinear Schrödinger (NLS) equations is still an open topic. NLS equations have received particular attention for describing nonlinear waves in optical fibres, photonics, plasmas, Bose–Einstein condensates and deep ocean. This work deals with rogue wave solutions of the chiral NLS equation. We introduce an inhomogeneous one-dimensional version, and using the similarity transformation and direct ansatz, we solve the equation in the presence of dispersive and nonlinear coupling which are modulated in time and space. As a result, we show how a simple choice of some free functions can display a lot of interesting rogue wave structures and the interaction of quantum rogue waves. The results obtained may give the possibility of conducting relevant experiments in quantum mechanics and achieving potential applications.

Keywords. Rogue waves; chiral nonlinear Schrödinger equation; modulated coefficients; quantum mechanics.

PACS Nos 05.45.Yv; 47.35.Fg; 02.30.Jr

1. Introduction

Nowadays, the study of rogue waves attracts a great deal of interest from scientific community, especially in nonlinear sciences. Rogue waves are giant single waves that may suddenly appear in oceans [1]. These are also known as monstrous waves, deadly waves or extreme waves. Their appearance can be quite unexpected and their origin is mysterious. The rogue wave phenomenon becomes more and more popular for describing nonlinear waves in other fields such as in nonlinear optics [2–4] and atmosphere [5], just to cite a few. Contrary to the dispersive behaviour adopted by traditional waves of low amplitude, rogue waves are self-reinforcing packets of solitary waves. The rogue wave phenomenon is not just a spectacular event accessible to routine observations and satellite images but also a combination of complex physical processes that occur under the accuracy conditions [6]. This complex combination of physical processes can be well described by the nonlinear Schrödinger (NLS) equations.

NLS equations are prototypical dispersive nonlinear partial differential equations which have been derived and analysed in various branches of physics such as nonlinear optics [7], photonics [8], Bose–Einstein condensates [9] and nonlinear oceanography [10,11]. It has been found that rogue waves are analytical solutions of some integrable NLS equations [12–15], Benjamin–Ono equation [16] and Hirota equation [17].

In recent years, it has been shown that the nonuniform physical systems are more suitable candidates for achieving the required controlling mechanisms [18]. The physical medium with defects or inhomogeneities always has some irregular changes, which are related to the realistic understanding of the nonlinear phenomena [19]. Along the same idea, experiment has shown that the inhomogeneity of a medium plays an important role in the generation of optical rogue waves, and the inhomogeneity is usually described by nonlinear differential equations with variable or inhomogeneity coefficients [20].

Many works have been devoted to the construction of analytical solutions of the NLS equations with inhomogeneity coefficients [21–26], and the results revealed that the generation of rogue waves can be well controlled through the management and the choice of variable coefficients [23–26].

Although significant progress has been made in that sense, it remains really difficult to relate all the characteristics of rogue waves to a specific NLS model equation. Motivated by these considerations, our aim in this work is to present a systematic theoretical study

Published online: 18 December 2019

for considering inhomogeneity coefficients in the chiral NLS equation and explore the effect of inhomogeneities of the underlying dynamics. The chiral NLS equation plays a fundamental role in developing quantum mechanics, especially in the field of quantum Hall effect, where chiral excitations are known to appear. In this paper, we consider the inhomogeneous chiral NLS equation of the form

$$\frac{\partial\psi}{\partial t}+\beta(t,x)\frac{\partial^2\psi}{\partial x^2}-i\sigma(t,x)\times\left(\psi^*\frac{\partial\psi}{\partial x}-\psi\frac{\partial\psi^*}{\partial x}\right)\psi=0, \tag{1}$$

where $\psi\equiv\psi(t,x)$ is the complex function of space x and time t. The parameter $\beta(t,x)$ is the dispersion coefficient and $\sigma(t,x)$ is the nonlinear coupling coefficient. The symbol * refers to the complex conjugate. The particular case, when $\beta(t,x)$ and $\sigma(t,x)$ are constant coefficients, was studied in [27–30] where both bright and dark soliton solutions were investigated. In this work, we investigate the analytical rogue wave solutions of the inhomogeneous chiral NLS equation (1).

The rest of the paper is organised as follows: In §2, we investigate the first-order and second-order rational-like solutions as the rogue wave solutions of eq. (1) using direct ansatz and by applying similarity transformations [23,25,31]. In §3, the paper ends with the summary of the results achieved.

2. Similarity transformations and rogue wave solutions

We consider the inhomogeneous chiral NLS equation (1). In order to investigate its analytical rogue wave solutions, we first assume the function $\psi(t,x)$ in the following form [23,25,31]:

$$\psi(t,x)=[\phi_{\mathrm{R}}(t,x)+i\phi_{\mathrm{I}}(t,x)]\mathrm{e}^{i\varphi(t,x)}, \tag{2}$$

where $\phi_{\mathrm{R}}(t,x)$ and $\phi_{\mathrm{I}}(t,x)$ are the real part and the imaginary part of $\psi(t,x)$, respectively. The function $\varphi(t,x)$ is the phase. Introducing eq. (2) into eq. (1), we obtain the following system of equations:

$$\begin{aligned}&\phi_{\mathrm{R},t}-\varphi_t\phi_{\mathrm{I}}+\frac{\beta(t,x)}{2}[\phi_{\mathrm{I},xx}+2\varphi_x\phi_{\mathrm{R},x}-\varphi_x^2\phi_{\mathrm{I}}\\&+\varphi_{xx}\phi_{\mathrm{R}}]+2\sigma(t,x)[\phi_{\mathrm{I}}\phi_{\mathrm{R}}\phi_{\mathrm{I},x}+\varphi_x\phi_{\mathrm{I}}^3\\&-\phi_{\mathrm{I}}^2\phi_{\mathrm{R},x}+\varphi_x\phi_{\mathrm{I}}\phi_{\mathrm{R}}^2]=0,\end{aligned} \tag{3a}$$

$$\begin{aligned}&-\phi_{\mathrm{I},t}-\varphi_t\phi_{\mathrm{R}}+\frac{\beta(t,x)}{2}[\phi_{\mathrm{R},xx}-2\varphi_x\phi_{\mathrm{I},x}-\varphi_x^2\phi_{\mathrm{R}}\\&-\varphi_{xx}\phi_{\mathrm{I}}]+2\sigma(t,x)[-\phi_{\mathrm{I}}\phi_{\mathrm{R}}\phi_{\mathrm{R},x}+\varphi_x\phi_{\mathrm{R}}^3\\&+\phi_{\mathrm{R}}^2\phi_{\mathrm{I},x}+\varphi_x\phi_{\mathrm{R}}\phi_{\mathrm{I}}^2]=0.\end{aligned} \tag{3b}$$

Introducing the new variables $\eta(t,x)$ and $\tau(t,x)$, we further utilise the following similarity transformations for the real functions $\phi_{\mathrm{R}}(t,x)$, $\phi_{\mathrm{I}}(t,x)$ and the phase $\varphi(t,x)$:

$$\begin{aligned}&\phi_{\mathrm{R}}(t,x)=A(t)+B(t)P(\eta(t,x),\tau(t)),\\&\phi_{\mathrm{I}}(t,x)=C(t)Q(\eta(t,x),\tau(t)),\\&\varphi(t,x)=\chi(t,x)+\mu\tau(t),\end{aligned} \tag{4}$$

where μ is a constant and the real variables $\eta(t,x)$, $\chi(t,x)$, $P(\eta,\tau)$, $Q(\eta,\tau)$, $\tau(t)$, $A(t)$, $B(t)$ and $C(t)$ will be determined later. Introducing (4) into (3), we obtain

$$\begin{aligned}&A_t+B_tP+B\eta_tP_\eta+B\tau_tP_\tau-(\chi_t+\mu\tau_t)CQ\\&+\frac{\beta(t,x)}{2}[C\eta_{xx}Q_\eta+C\eta_x^2Q_{\eta\eta}+2\chi_x\eta_xBP_\eta\\&-\chi_x^2CQ+\chi_{xx}(A+PB)]\\&+2\sigma(t,x)([(A+PB)Q_\eta-BQP_\eta]C^2Q\eta_x\\&+\chi_xCQ[(CQ)^2+(A+PB)^2])=0,\end{aligned} \tag{5a}$$

$$\begin{aligned}&-C_tQ-C\eta_tQ_\eta-C\tau_tQ_\tau-(\chi_t+\mu\tau_t)(A+PB)\\&+\frac{\beta(t,x)}{2}[B\eta_{xx}P_\eta+B\eta_x^2P_{\eta\eta}-2\chi_x\eta_xCQ_\eta\\&-\chi_x^2(A+PB)-\chi_{xx}(CQ)]\\&+2\sigma(t,x)([(A+PB)Q_\eta-BQP_\eta]C(A+PB)\eta_x\\&+\chi_x(A+PB)[(CQ)^2+(A+PB)^2])=0.\end{aligned} \tag{5b}$$

From (5), we obtain the following similarity reductions:

$$\eta_{xx}=0, \tag{6a}$$

$$2\chi_t+\beta(t,x)\chi_x^2=0, \tag{6b}$$

$$\eta_t+\beta(t,x)\eta_x\chi_x=0, \tag{6c}$$

$$2\theta_t+\beta(t,x)\chi_{xx}\theta=0,\quad\theta=A,B,C, \tag{6d}$$

$$(A+PB)Q_\eta-BQP_\eta=0, \tag{6e}$$

$$\begin{aligned}&B\tau_tP_\tau-\mu\tau_tCQ+\frac{\beta(t,x)}{2}C\eta_x^2Q_{\eta\eta}\\&+2\sigma(t,x)\chi_xCQ[(CQ)^2+(A+PB)^2]=0,\end{aligned} \tag{6f}$$

$$\begin{aligned}&-C\tau_tQ_\tau-\mu\tau_t(A+PB)+\frac{\beta(t,x)}{2}B\eta_x^2P_{\eta\eta}\\&+2\sigma(t,x)\chi_x(A+PB)[(CQ)^2+(A+PB)^2]=0.\end{aligned} \tag{6g}$$

After some calculation, we obtain from eqs (6a)–(6d) the following equations:

$$\eta(t,x)=\alpha(t)x+\delta(t),\quad A(t)=a_0\sqrt{|\alpha(t)|},$$
$$\chi(t,x)=-\frac{\alpha_t}{2\beta(t,x)\alpha(t)}x^2-\frac{\delta_t}{2\beta(t,x)\alpha(t)}x+\chi_0(t),$$
$$B(t)=bA(t),\quad C(t)=cA(t), \tag{7}$$

where a_0, b and c are arbitrary constants, $\alpha(t)$ is the inverse of the wave width, and $\delta(t)$ and $\chi_0(t)$ are free functions of time t.

Proceeding to a more advanced reduction of eqs (6e)–(6g), we end up with a system of partial differential equations with constant coefficients and for that, we require the conditions

$$\tau_t=\frac{\beta(t,x)}{2}\eta_x^2\quad\text{and}\quad\sigma(t,x)=\frac{\beta(t,x)}{4}\frac{\eta_x^2}{\chi_x}GA^{(-2)}.$$

This can generate the constraints for the variable $\tau(t)$ and the nonlinearity coefficient $\sigma(t,x)$:

$$\tau(t)=\frac{1}{2}\int_0^t\alpha^2(u)\beta(u)\,\mathrm{d}u,$$
$$\sigma(t,x)=-\frac{G\beta^2(t,x)\alpha^2(t)}{4a_0^2(\alpha_t x+\delta_t)}. \tag{8}$$

Replacing the expressions of τ_t and $\sigma(t,x)$ given in (8), we obtain from eqs (6f) and (6g) the following coupled system of differential equations with constant coefficients:

$$bP_\tau-\mu cQ+cQ_{\eta\eta}+cGQ[(cQ)^2+(1+bP)^2]=0, \tag{9a}$$
$$-cQ_\tau-\mu(1+pB)+bP_{\eta\eta}+G(1+bP)[(cQ)^2+(1+bP)^2]=0. \tag{9b}$$

2.1 *First-order rational-like solution*

The first-order rational solution of (9) is obtained following [12,13,23,25]. It follows from (9) that we have the solutions

$$P(\eta,\tau)=-\frac{4}{bH_1(\eta,\tau)}$$

and

$$Q(\eta,\tau)=-\frac{8\tau}{cH_1(\eta,\tau)}$$

with $H_1(\eta,\tau)=1+2\eta^2+4\tau^4$ for $\mu=G=1$. Then, the first-order rational-like solution of (1) can be written as

$$\psi_1(t,x)=a_0\sqrt{|\alpha(t)|}\times\left[1-\frac{4+8i\tau(t)}{1+2[\alpha(t)x+\delta(t)]^2+4\tau^2}\right]\times e^{i[\chi(t,x)+\tau(t)]}, \tag{10}$$

where $\chi(t,x)$ and $\tau(t)$ are given by (7) and (8) respectively. Its intensity is given by the relation

$$|\psi_1(t,x)|^2=a_0^2|\alpha(t)|\frac{\{2[\alpha(t)x+\delta(t)]^2+4\tau^2-3\}^2+64\tau^2}{\{1+2[\alpha(t)x+\delta(t)]^2+4\tau^2\}^2}. \tag{11}$$

Let us choose some free functions of time to exhibit the obtained rational-like solution (10) for the fixed parameters $\alpha_0=1$ and $\chi_0(t)=0$. For simplicity, we choose the functions β and σ as modulated only in time or both in time and space depending on the expected behaviour.

(i) The free functions are chosen as polynomials of time t, i.e. $\alpha(t)=1$, $\beta(t)=t^2/2$. Figures 1a–1d present the behaviour of rational solution (10) for different terms $\delta(t)=t,t^2$, respectively, for which the coefficient $\sigma(t,x)\equiv\sigma(t)$ in eq. (1) is given by

$$\sigma(t)=-\frac{t^6}{16}\quad\text{for }\delta(t)=t, \tag{12a}$$

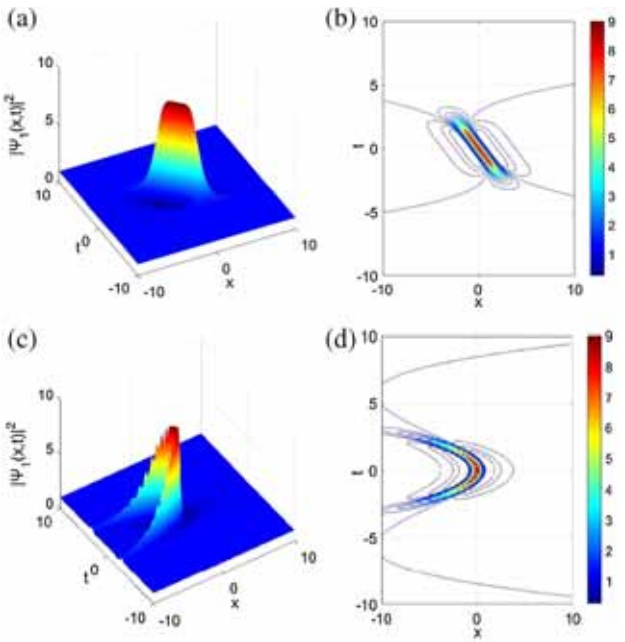

Figure 1. Rogue wave propagations (left column) with dromion structure (**a**), chirped structure (**c**) and the corresponding contour plots (right column), respectively, for the intensity $|\psi_1(t,x)|^2$ of the first-order rational solution (10) for $a_0=1$, $\alpha(t)=1$, $\beta(t)=0.5t^2$. (**a**) and (**b**) $\delta(t)=t$ and (**c**) and (**d**) $\delta(t)=t^2$.

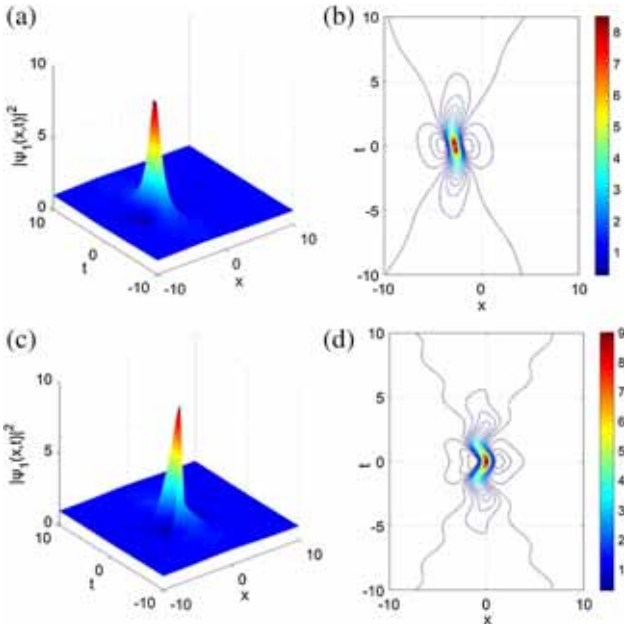

Figure 2. Rogue wave propagations (left column) with dromion structure and contour plots (right column), for the intensity $|\psi_1(t,x)|^2$ of the first-order rational solution (10) for $a_0 = 1$, $\alpha(t) = 1$, $\beta(t) = \cos^2(0.02t)$. (**a**) and (**b**) $\delta(t) = \mathrm{e}^{(1+0.1\,\sin(t))}$ and (**c**) and (**d**) $\delta(t) = \sin^2(t)$.

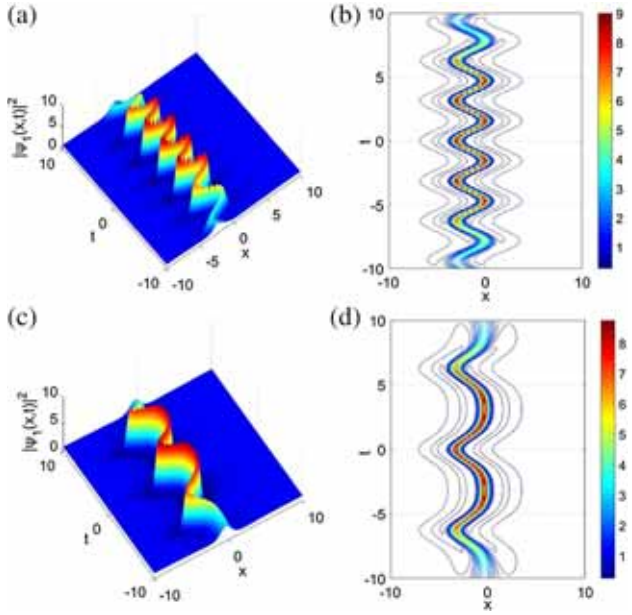

Figure 3. Rogue wave propagations with chirped structure and snaking behaviour (left column) and contour plots (right column), for the intensity $|\psi_1(t,x)|^2$ of the first-order rational solution (10) for $a_0 = 1.0$, $\alpha(t) = 1$, $\beta(t) = \sin^2(0,08t)$. (**a**) and (**b**) $\delta(t) = 3\cos^2(t)$ and (**c**) and (**d**) $\delta(t) = \mathrm{e}^{1.2\,\cos(t)}$.

$$\sigma(t) = -\frac{t^5}{32} \quad \text{for } \delta(t) = t^2. \tag{12b}$$

For $\alpha(t) = 1$, $\delta(t) = t$ and $\beta(t) = t^2/2$, figures 1a and 1b show a rogue wave with the dromion structure. When $\alpha(t) = 1$, $\delta(t) = t^2$ and $\beta(t) = t^2/2$, we have the propagation of a rogue wave with chirped structure in the same symmetric time interval (figures 1c and 1d).

(ii) The free functions are chosen as periodic functions of time such as trigonometric functions, i.e. $\alpha(t) = 1$, $\beta(t) = \cos^2(0.02t)$. Figures 2a–2d show the behaviour of rational solution (12) for different terms $\delta(t) = \mathrm{e}^{(1+0.1\,\sin(t))}$, $\sin^2(t)$, respectively, for which the coefficient $\sigma(t)$ in eq. (1) is given by

$$\sigma(t) = -10\frac{\cos^4(t/50)}{\cos(t)\mathrm{e}^{(1+0.1\,\sin(t))}} \quad \text{for } \delta(t) = \mathrm{e}^{(1+0.1\,\sin(t))}, \tag{13a}$$

$$\sigma(t) = -\frac{\cos^4(t/50)}{8\cos(t)\sin(t)} \quad \text{for } \delta(t) = \sin^2(t). \tag{13b}$$

For $\alpha(t) = 1$, $\delta(t) = \mathrm{e}^{(1+0.1\,\sin(t))}$ or $\delta(t) = \sin^2(t)$ and $\beta(t) = \cos^2(0.02t)$, figures 2a–2d show the rogue wave propagations with the dromion structures.

(iii) The free functions are chosen as periodic functions of time such as trigonometric functions, i.e. $\alpha = 1$ and $\beta(t) = \sin^2(0.08t)$. Figures 3a–3d show the behaviour of rational solution (12) for different terms $\delta(t) = 3\cos^2(t)$, $\mathrm{e}^{(1.2\cos(t))}$, respectively, for which the coefficient $\sigma(t)$ in eq. (1) is given by

$$\sigma(t) = \frac{\sin^4(2t/25)}{24\sin(t)\cos(t)} \quad \text{for } \delta(t) = 3\cos^2(t), \tag{14a}$$

$$\sigma(t) = \frac{\sin^4(2t/25)}{4.8\sin(t)\mathrm{e}^{1.2\cos(t)}} \quad \text{for } \delta(t) = \mathrm{e}^{(1.2\cos(t))}. \tag{14b}$$

For $\alpha(t) = 1$, $\delta(t) = 3\cos^2(t)$ or $\delta(t) = \mathrm{e}^{(1.2\cos(t))}$ and $\beta(t) = \sin^2(0.08t)$, we have chirping rogue structures with snaking behaviour propagating along the t-axis (figures 3a–3d).

(iv) The free functions are chosen as periodic functions of time such as Jacobian elliptic functions, i.e. $\alpha(t)=dn(t,m)$ and $\beta(t)=cn(t,m)$, where m is the module. Figures 4a–4d show the behaviour of rational solution (10) for different terms $\delta(t) = sn(t,m)$, $cn(t,m)$, respectively, for which the coefficient $\sigma(t,x)$ in eq. (1) is given by

$$\sigma(t,x) = -\frac{cn(t,m)dn^2(t,m)}{4\left[-xm^2sn(t,m) + dn(t,m)\right]} \quad \text{for } \delta(t) = sn(t,m), \tag{15a}$$

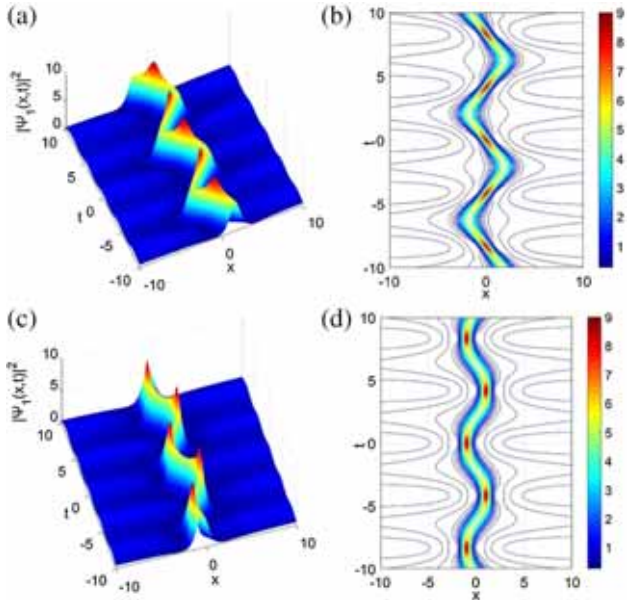

Figure 4. Rogue wave propagations with chirped structure and snaking behaviour (left column) and contour plots (right column), for the intensity $|\psi_1(t,x)|^2$ of the first-order rational solution (10) for $a_0 = 1.0, \alpha(t) = dn(t,m), \beta(t) = cn(t,m)$. (**a**) and (**b**) $\delta(t) = sn(t,m)$ and (**c**) and (**d**) $\delta(t) = cn(t,m)$, with $m = 0.707$.

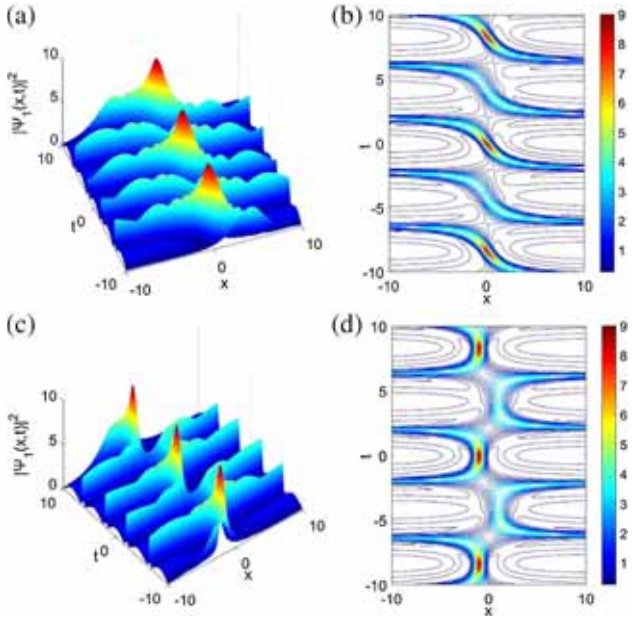

Figure 5. Periodic rogue wave propagations with chirped structure (left column) and contour plots (right column), for the intensity $|\psi_1(t,x)|^2$ of the first-order rational solution (10) for $a_0 = 1.0$, $\alpha(t) = cn(t,m)$, $\beta(t) = dn(t,m)$. (**a**) and (**b**) $\delta(t) = sn(t,m)$ and (**c**) and (**d**) $\delta(t) = dn(t,m)$, with $m = 0.707$.

$$\sigma(t,x) = \frac{cn^2(t,m)dn^2(t,m)}{4sn(t,m)[xm^2cn(t,m) + dn(t,m)]} \quad \text{for } \delta(t) = cn(t,m). \tag{15b}$$

For $\alpha(t)$=$dn(t,m)$, $\delta(t)$=$sn(t,m)$ or $\delta(t)$=$cn(t,m)$ and $\beta(t) = cn(t,m)$, where $m = 0.707$, we have chirping rogue structures with snaking behaviour propagating along the t-axis (figures 4a–4d).

(v) The free functions are chosen as periodic functions of time such as Jacobian elliptic functions, i.e. $\alpha(t) = cn(t,m)$ and $\beta(t) = dn(t,m)$. Figures 5a–5d give the behaviour of rational solution (10) for different terms $\delta(t) = sn(t,m), dn(t,m)$, respectively, for which the coefficient $\sigma(t,x)$ in eq. (1) is given by

$$\sigma(t,x) = -\frac{dn(t,m)cn^2(t,m)}{4[-xsn(t,m) + cn(t,m)]} \quad \text{for } \delta(t) = sn(t,m), \tag{16a}$$

$$\sigma(t,x) = \frac{cn^2(t,m)dn^2(t,m)}{4sn(t,m)[xdn(t,m) + m^2cn(t,m)]} \quad \text{for } \delta(t) = dn(t,m). \tag{16b}$$

For $\alpha(t)$=$cn(t,m)$, $\delta(t)$=$sn(t,m)$ or $\delta(t)$=$dn(t,m)$ and $\beta(t)$=$dn(t,m)$, where m=0.707, figures 5a–5d show periodic rogue waves with chirped structures.

2.2 *Second-order rational-like solution*

In this case, we have [12,13,23,25]

$$P(\eta,\tau) = \frac{R_2(\eta,\tau)}{bH_2(\eta,\tau)}$$

and

$$Q(\eta,\tau) = \frac{B_2(\eta,\tau)}{cH_2(\eta,\tau)},$$

where

$$\begin{aligned} H_2(\eta,\tau) &= \frac{1}{12}\eta^6 + \frac{1}{2}\eta^4\tau^2 + \eta^2\tau^4 + \frac{2}{3}\tau^6 + \frac{1}{8}\eta^4 \\ &\quad + \frac{9}{2}\tau^4 - \frac{3}{2}\eta^2\tau^2\frac{9}{16}\eta^2 + \frac{33}{8}\tau^2 + \frac{3}{32}, \\ R_2(\eta,\tau) &= -\frac{1}{2}\eta^4 - 6\eta^2\tau^2 - 10\tau^4 \\ &\quad - \frac{3}{2}\eta^2 - 9\tau^2 + \frac{3}{8}, \\ B_2(\eta,\tau) &= -\tau\left[\eta^4 + 4\eta^2\tau^2 + 4\tau^4 - 3\eta^2 + 2\tau^2 - \frac{15}{4}\right]. \end{aligned} \tag{17}$$

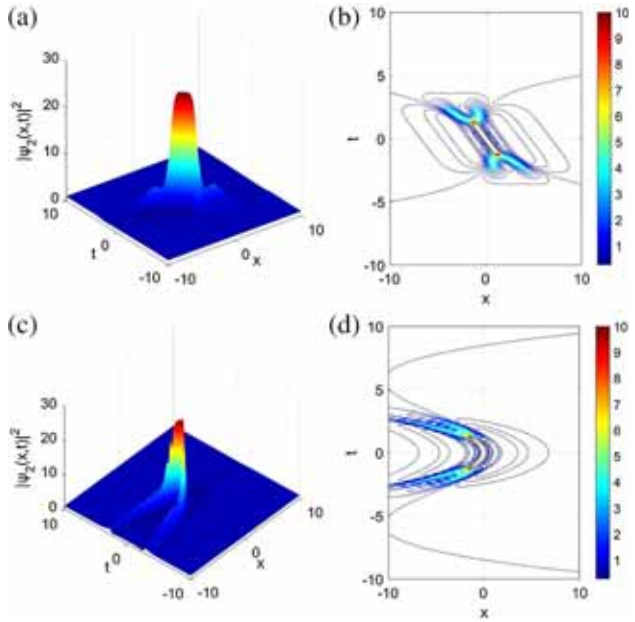

Figure 6. Rogue wave propagations (left column) with dromion structure (**a**), chirped structure (**c**) and the corresponding contour plots (right column), respectively, for the intensity $|\psi_2(t,x)|^2$ of the second-order rational solution (18) for $a_0 = 1.0$, $\alpha(t) = 1$, $\beta(t) = 0.5t^2$. (**a**) and (**b**) $\delta(t) = t$ and (**c**) and (**d**) $\delta(t) = t^2$.

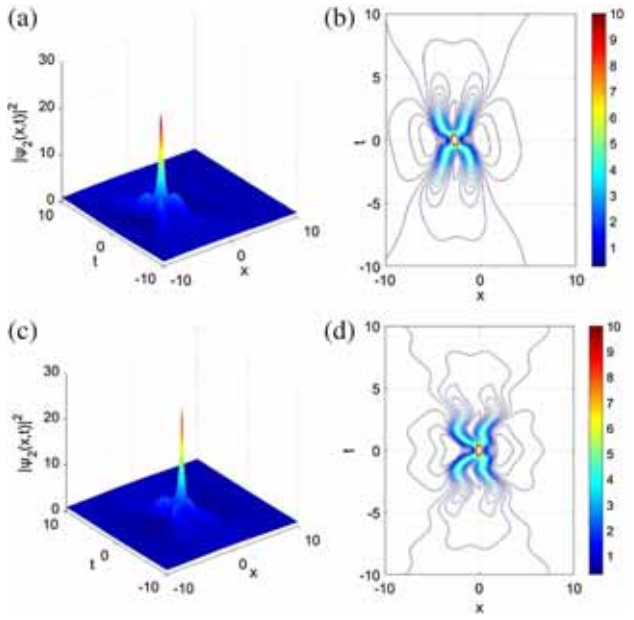

Figure 7. Rogue wave propagations (left column) with dromion structure and contour plots (right column), for the intensity $|\psi_2(t,x)|^2$ of the second-order rational solution (18) for $a_0 = 1.0$, $\alpha(t) = 1$, $\beta(t) = \cos^2(0.02t)$. (**a**) and (**b**) $\delta(t) = \mathrm{e}^{(1+0.1\sin(t))}$ and (**c**) and (**d**) $\delta(t) = \sin^2(t)$.

On the basis of similarity transformations, we obtain the second-order rational solution of eq. (1) in the following form:

$$\psi_2(t,x) = a_0\sqrt{|\alpha(t)|}\left[1 - \frac{R_2(\eta,\tau) + iB_2(\eta,\tau)}{H_2(\eta,\tau)}\right] \times \mathrm{e}^{i[\chi(t,x)+\tau(t)]}, \tag{18}$$

where the intensity is given by

$$|\psi_2(t,x)|^2 = a_0^2|\alpha(t)|\frac{[H_2(\eta,\tau) + R_2(\eta,\tau)]^2 + B_2^2(\eta,\tau)}{H_2^2(\eta,\tau)}. \tag{19}$$

Here $\eta \equiv \eta(t,x)$, $\tau \equiv \tau(t)$ and $\chi \equiv \chi(t,x)$.

The corresponding behaviour of second-order rational solution is illustrated in figures 6–10 for the fixed parameters $\alpha_0 = 1$ and $\chi_0(t) = 0$. We choose: (i) $\alpha(t) = 1$, $\beta(t) = t^2/2$and $\delta(t) = t, t^2$ in figures 6a–6d, (ii) $\alpha(t) = 1, \beta(t) = \cos^2(0.02t)$ and $\delta(t) = \mathrm{e}^{(1+0.1\sin(t))}$, $\sin^2(t)$ in figures 7a–7d, (iii) $\alpha(t) = 1$, $\beta(t) = \sin^2(0.02t)$ and $\delta(t) = 3\cos^2(t), \mathrm{e}^{1.2\cos(t)}$ in figures 8a–8d, (iv) $\alpha(t) = dn(t,m)$, $\beta(t) = cn(t,m)$ and $\delta(t) = sn(t,m)$, $cn(t,m)$ in figures 9a–9d and (v) $\alpha(t) = cn(t,m)$, $\beta(t) = dn(t,m)$, and $\delta(t) = sn(t,m), dn(t,m)$ in figures 10a–10d.

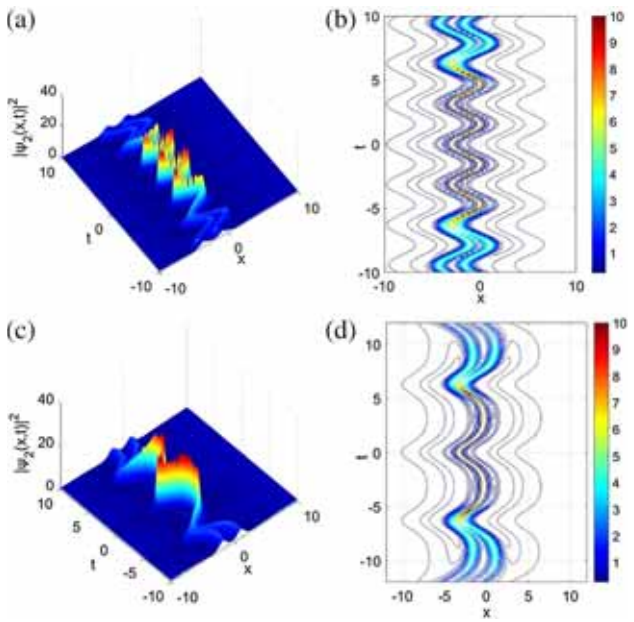

Figure 8. Rogue wave propagations with chirped structure and snaking behaviour (left column) and contour plots (right column), for the intensity $|\psi_2(t,x)|^2$ of the second-order rational solution (18) for $a_0 = 1.0$, $\alpha(t) = 1$, $\beta(t) = \sin^2(0,08t)$. (**a**) and (**b**) $\delta(t) = 3\cos^2(t)$ and (**c**) and (**d**) $\delta(t) = \mathrm{e}^{1.2\cos(t)}$.

Figures 6–10 show that although the same functions, as those in figures 1–5, are chosen respectively, the waves have double structures compared to the

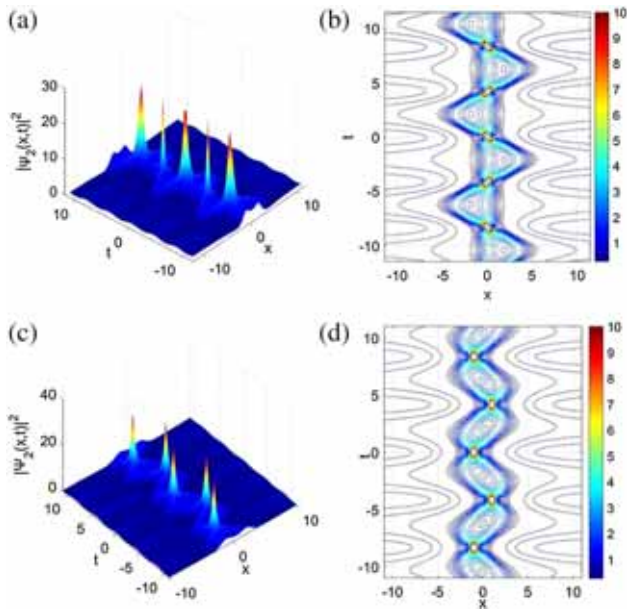

Figure 9. Rogue wave propagations with dromion structure and snaking behaviour (left column) and contour plots (right column), for the intensity $|\psi_2(t,x)|^2$ of the second-order rational solution (18) for $a_0 = 1.0$, $\alpha(t) = dn(t,m)$, $\beta(t) = cn(t,m)$. (**a**) and (**b**) $\delta(t) = sn(t,m)$ and (**c**) and (**d**) $\delta(t) = cn(t,m)$, with $m = 0.707$.

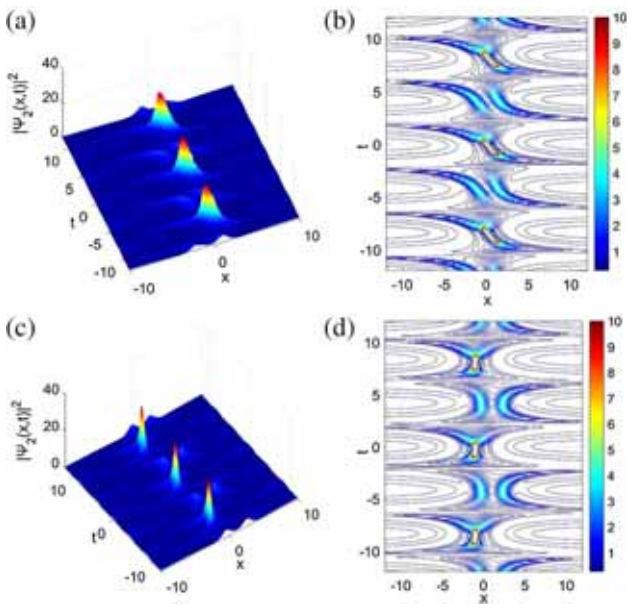

Figure 10. Periodic rogue waves with dromion structure (left column) and contour plots (right column), for the intensity $|\psi_2(t,x)|^2$ of the second-order rational solution (18) for $a_0 = 1.0$, $\alpha(t) = cn(t,m)$, $\beta(t) = dn(t,m)$. (**a**) and (**b**) $\delta(t) = sn(t,m)$ and (**c**) and (**d**) $\delta(t) = dn(t,m)$, with $m = 0.707$.

former single ones, and now with higher amplitude. Similar behaviours have been found in [12]. Furthermore, figures 6–10 depict the fascinating dynamical interactions of modified rogue waves known as rogons [23].

3. Conclusion

In this work, we presented the analytical solutions in terms of rational-like functions of the chiral nonlinear Schrödinger equation with inhomogeneous coefficients using a similarity transformation and a direct ansatz. We obtained the first and second order of rational solutions. In particular, by choosing some free functions of time, we showed that the system can exhibit the snake propagation traces and the fascinating interactions of modified rogue waves known as rogons [23]. The results obtained in this paper are similar to those found on the possible formation mechanisms for the optical rogue wave phenomenon in optical fibres, the oceanic rogue wave phenomenon in the deep ocean and the matter rogue wave phenomenon in Bose–Einstein condensates. To date, chiral effects have been almost completely ignored in efforts to explain the possible formation mechanism of rogue waves in some inhomogeneous NLS equation. The results presented in this paper may be important to describe the possible formation mechanisms for rogue wave phenomenon in the development of quantum mechanics.

Acknowledgements

The authors thank the anonymous referees for a careful reading of the paper and constructive suggestions, which helped to improve the paper.

References

[1] P Müller, C Garrett and A Osbone, *Oceanography* **18**, 66 (2005)
[2] D R Solli, C Ropers, P Koonath and B Jalali, *Nature* **450**, 1054 (2007)
[3] A Montina, U Bortolozzo, S Residori and F T Arecchi, *Phys. Rev. Lett.* **103**, 173901 (2009)
[4] H P Chai, B Tian, J Chai and D Zhong, *Pramana – J. Phys.* **92**: 9 (2019)
[5] L Stenflo and M Marklund, *J. Plasma Phys.* **76**, 293 (2010)
[6] C B Mbane, *Int. J. Phys. Sci.* **8**, 1284 (2013)
[7] Y S Kivshar and G Agrawal, *Optical solitons: From fibers to photonic crystals* (Academic Press, San Diego, 2003)
[8] A Hasegawa, *Optical solitons in fibers* (Springer, Berlin, 1989) pp. 1–74

[9] F Dalfovo, S Giorgini, L P Pitaevskii and S Stringari, *Rev. Mod. Phys.* **71**, 463 (1999)
[10] M Onorato, A R Osborne, M Serio and S Bertone, *Phys. Rev. Lett.* **86**, 5831 (2001)
[11] C Kharif, E Pelinovsky and A Slunyaey, *Rogue waves in the ocean: Observation, theories and modeling* (Springer, New York, 2009)
[12] N Akhmediev, A Ankiewicz and J M Soto-Crespo, *Phys. Rev. E* **80**, 026601 (2009)
[13] N Akhmediev, J M Soto-Crespo and A Ankiewicz, *Phys. Lett. A* **373**, 2137 (2009)
[14] N Akhmediev, J M Soto-Crespo and A Ankiewicz, *Phys. Rev. A* **80**, 043818 (2009)
[15] K L Henderson, D H Peregrine and J W Dold, *Wave Motion* **29**, 341 (1999)
[16] Y K Liu and B Li, *Pramana – J. Phys.* **88**: 57 (2017)
[17] H Gao, *Pramana – J. Phys.* **88**: 84 (2017)
[18] T Yong-Sheng, H Jing-Song and K Porsezian, *Chin. Phys. B* **88**, 074210 (2013)
[19] F Abdullaev, *Theory of solitons in inhomogeneous media* (Wiley, New York, 1994)
[20] F T Arecchi, U Bortolozzo, A Montina and S Residori, *Phys. Rev. Lett.* **106**, 153901 (2011)
[21] V N Serkin, T L Belyaeva, I V Alexandrov and G Me Melchor, *Int. Soc. Optics Photon.* **4271**, 292 (2001)
[22] K Senthilnathan, Q Li, K Nakkeeran and P K A Wai, *Phys. Rev. A* **78**, 033835 (2008)
[23] Z Yan, *Phys. Lett. A* **374**, 672 (2010)
[24] W P Zhong, M R Belic and T Huang, *Phys. Rev. E* **87**, 065201 (2013)
[25] Z-Y Ma and S-H Ma, *Chin. Phys. B* **21**, 03050 (2012)
[26] C Liu, Y Y Li, M Gao, Z Wang, Z Dai and C Wang, *Pramana – J. Phys.* **85**, 1063 (2015)
[27] M Younis, N Cheemaa, S A Mahmood and S T R Rizvi, *Opt. Quant. Electron.* **48**, 542 (2016)
[28] H Bulut, T A Sulaiman and B Demirdag, *Nonlinear Dyn.* **91**, 1985 (2018)
[29] A Nishino, Y Umeno and M Wadati, *Chaos Solitons Fractals* **9**, 1063 (1998)
[30] G Ebadi, A Yildirim and A Biswas, *Rom. Rep. Phys.* **64**, 357 (2012)
[31] V M Perez-Garcıa, P J Torres and V V Konotop, *Physica D* **221**, 31 (2006)